Nuclear Engineering and Technology 54 (2022) 842–848

Contents lists available at ScienceDirect

Nuclear Engineering and Technology

journal homepage: www.elsevier.com/locate/net

Original article

Heat transfer analysis in sub-channels of rod bundle geometry with supercritical water

Edward Shitsi [a, c, *], Seth Kofi Debrah [a, b], Silas Chabi [a], Emmanuel Maurice Arthur [a], Isaac Kwasi Baidoo [c]

[a] Department of Nuclear Engineering, Graduate School of Nuclear and Allied Sciences, University of Ghana, Accra, AE 1, Ghana
[b] Nuclear Power Institute, Ghana Atomic Energy Commission GAEC, P.O. Box LG 80, Legon, Accra, Ghana
[c] National Nuclear Research Institute, Ghana Atomic Energy Commission GAEC, P.O. Box LG 80, Legon, Accra, Ghana

ARTICLE INFO

Article history:
Received 5 March 2021
Received in revised form
24 May 2021
Accepted 24 September 2021
Available online 27 September 2021

Keywords:
Fuel assembly
Sub-channels
Heat transfer
Computational fluid dynamics
Supercritical water cooled reactor

ABSTRACT

Parametric studies of heat transfer and fluid flow are very important research of interest because the design and operation of fluid flow and heat transfer systems are guided by these parametric studies. The safety of the system operation and system optimization can be determined by decreasing or increasing particular fluid flow and heat transfer parameter while keeping other parameters constant. The parameters that can be varied in order to determine safe and optimized system include system pressure, mass flow rate, heat flux and coolant inlet temperature among other parameters. The fluid flow and heat transfer systems can also be enhanced by the presence of or without the presence of particular effects including gravity effect among others. The advanced Generation IV reactors to be deployed for large electricity production, have proven to be more thermally efficient (approximately 45% thermal efficiency) than the current light water reactors with a thermal efficiency of approximately 33 °C. SCWR is one of the Generation IV reactors intended for electricity generation. High Performance Light Water Reactor (HPLWR) is a SCWR type which is under consideration in this study. One-eighth of a proposed fuel assembly design for HPLWR consisting of 7 fuel/rod bundles with 9 coolant sub-channels was the geometry considered in this study to examine the effects of system pressure and mass flow rate on wall and fluid temperatures. Gravity effect on wall and fluid temperatures were also examined on this one-eighth fuel assembly geometry. Computational Fluid Dynamics (CFD) code, STAR-CCM+, was used to obtain the results of the numerical simulations. Based on the parametric analysis carried out, sub-channel 4 performed better in terms of heat transfer because temperatures predicted in sub-channel 9 (corner sub-channel) were higher than the ones obtained in sub-channel 4 (central sub-channel). The influence of system mass flow rate, pressure and gravity seem similar in both sub-channels 4 and 9 with temperature distributions higher in sub-channel 9 than in sub-channel 4. In most of the cases considered, temperature distributions (for both fluid and wall) obtained at 25 MPa are higher than those obtained at 23 MPa, temperature distributions obtained at 601.2 kg/h are higher than those obtained at 561.2 kg/h, and temperature distributions obtained without gravity effect are higher than those obtained with gravity effect. The results show that effects of system pressure, mass flowrate and gravity on fluid flow and heat transfer are significant and therefore parametric studies need to be performed to determine safe and optimum operating conditions of fluid flow and heat transfer systems.

1. Introduction

Parametric studies of heat transfer and fluid flow are very important research of interest because the design and operation of fluid flow and heat transfer systems are guided by these parametric studies. The safety of the system operation and system optimization can be determined by decreasing or increasing particular fluid

* Corresponding author. Department of Nuclear Engineering, Graduate School of Nuclear and Allied Sciences, University of Ghana, Accra, AE 1, Ghana.
E-mail addresses: edwardshitsi@yahoo.com (E. Shitsi), s.debrah@gaecgh.org (S.K. Debrah), engsilas89@gmail.com (S. Chabi), emarthur001@st.ug.edu.gh (E.M. Arthur), baidooisaac51@yahoo.co.uk (I.K. Baidoo).

https://doi.org/10.1016/j.net.2021.09.027

flow and heat transfer parameter while keeping other parameters constant. The parameters that can be varied in order to determine safe and optimized system include system pressure, mass flow rate, heat flux and coolant inlet temperature among other parameters. The fluid flow and heat transfer systems can also be enhanced by the presence of or without the presence of particular effects including gravity effect among others. The advanced Generation IV reactors to be deployed for large electricity production, have proven to be more thermally efficient (approximately 45% thermal efficiency) than the current light water reactors with a thermal efficiency of approximately 33 °C [1]. SCWR is one of the Generation IV reactors intended for electricity generation. High Performance Light Water Reactor HPLWR is a SCWR type which is under consideration in this study.

[2] performed a heat transfer study in a supercritical high-performance light water reactor (HPLWR) with the aim of improving heat transfer characteristics in the fuel assembly of HPLWR. Coupled codes, ANSYS-CFX-19.0 (CFD code) and MCNP6 (Monte Carlo neutronics code), were used for the study. Heat transfer deterioration (HTD) and non-uniform distribution of temperature on the surface of the cladding were observed in the fuel assembly. [1] carried out a review giving more details on the supercritical water-cooled reactor (SCWR) and its application in nuclear marine vessels which are currently operating with pressurized water-saturated steam nuclear power plants. It was proposed that SCWR design concept application for marine vessels would result in a significant reduction in plant size, weight, capital cost and operating cost. The need for further studies on SCWR application for marine vessels was recommended in this study in order to achieve this dream. [26] performed numerical study of heat transfer in a 61-rod bundle (fuel assembly) of SCWR. It was observed that the difference between minimum and maximum non-uniform wall temperatures on the surfaces of the fuel rods near the fuel assembly outlet was over 200 K, and this was caused by differences in the mass flow rates in the sub-channels of the fuel assembly. [3] carried out heat transfer numerical study in the 1000 MW supercritical boiler water-cooled wall tube. The numerical simulation method made use of RNG k- ε turbulence model and investigated effects of buoyancy, centrifugal force, flow deviation, inlet temperature deviation and specific heat on heat transfer. The variation of heat flux was done along the furnace height. The results of the study show that HTD is caused by buoyancy effect and decrease in thermal conductivity, and HTE is caused by centrifugal force and increase in inlet mass flow rate.

There are several other studies on heat transfer at supercritical pressures which are related to SCWR design concepts but few of these studies are on fuel/rod bundle geometry [4–18]. This study is the extension of the study performed by Ref. [19] to assess the performance of heat transfer correlations in the sub-channels of the adopted rod bundle geometry. The available literature has shown a lot of fluid flow and heat transfer studies performed in tube related geometries whereas there are limited studies performed in rod bundle geometries because modelling of rod bundle geometries is relatively complicated than that of tube related geometries. Currently there are no CFD study results on the research interest of fluid flow and heat transfer trying to find out whether temperature distributions in the various coolant sub-channels of the proposed geometry for HPLWR will be uniform or otherwise. In other words, it is important to find out the coolant sub-channels having lowest or highest temperature distributions using CFD methodology. Therefore, there is the need for more studies on fuel/rod bundle geometry at supercritical pressures depicting the real practical situation of design and operation of SCWRs. This study investigates the effects of parameters such as system pressure, mass flow rate and gravity on fluid flow and heat transfer at supercritical pressures in one-eighth of a proposed fuel assembly design for HPLWR which consists of 7 fuel/rod bundles with 9 coolant sub-channels. This study which intends to contribute to the existing knowledge on few studies on rod bundle geometry at supercritical pressures, also demonstrates the need to carry out parametric studies in order to determine the optimum operating conditions of fluid flow and heat transfer systems.

2. Methodology

The Methodology adopted by Ref. [19] in assessment of heat transfer correlations in the sub-channels geometry was also employed in this study. Computational Fluid Dynamics (CFD) code, STAR-CCM+, was used to obtain the results of the numerical simulations. STAR-CCM + CAD and the System Model Descriptions, Initial Conditions, and Physical Models considered in this work were already presented in the [19]. Mesh Scene of the Computational Geometry, and a representation of Fuel rod and sub-channels in "1/8 fuel assembly" created using STAR-CCM + CAD are shown in Fig. 1. The Optimum mesh size of 1, 177, 342 cells describing the sub-channel geometry was used for the study. Detailed dimensions of the 1/8th fuel assembly implemented in STAR-CCM + CAD is presented in Table 1. Physics models and boundary specifications presented in Table 1 in Ref. [19] were also adopted for this study. The fuel rods were heated with a uniform heat flux of 650 kW/m^2. The system pressures of 23 MPa and 25 MPa, mass flow rates of 0.1670 kg/s (601.2 kg/h) and 0.1559 kg/s (561.2 kg/h), and coolant inlet temperature of 300 °C were also adopted.

The Physical Models including Continuity, Momentum and Energy equations were also adopted in this study. Literatures by Refs. [20,21,23]; and [24] contained detailed descriptions of the Physical Models.

3. Results and discussion

3.1. Turbulence model selection and numerical Simulation/Wataa's results comparison

[25] used MCNP code to calculate the distribution of power in each fuel rod, which was subsequently imported into STAFAS code to get the equivalent thermal-hydraulic conditions in each sub-channel of the proposed HPLWR fuel assembly. In this work, the design and operating conditions of the fuel assembly were implemented in the STAR-CCM + code to obtain temperature distributions in the fuel assembly. The fuel assembly geometry used for both studies consists of 7 fuel rods and 9 sub-channels. The results of sub-channels 4 and 9 which are shown to have the lowest and highest coolant temperatures respectively are presented in this work. With the unavailability of the experimental data on the fuel assembly under consideration, the temperature distribution results of the STAFAS [25]) and STAR-CCM + codes were compared as a way of validating the results obtained in this work. Four (4) turbulence models including Shear-Stress Transport (SST) Menter's, κ-ω; Standard Wilcox, κ-ω; Abe-Kondoh-Nagano (AKN) Low-Re, κ-ε; and Standard Lien's Low-Re, κ-ε were compared in trying to obtain temperature distribution results of STAFAS code using STAR CCM + code. The symbols κ, ε, and ω respectively denote turbulent kinetic energy, dissipation rate and specific dissipation rate. The results of sub-channels 4 and 9 are shown respectively in Figs. 2 and 3. The wall temperatures (Tw) and coolant temperatures (Tcol) of the various turbulence models and that of Wataa's STAFAS code simulation are also shown in Figs. 2 and 3. The Tw and Tcol results of Shear-Stress Transport (SST) Menter's, κ-ω and Standard Wilcox, κ-ω turbulence models shown to be close and closely predicted the Wataa's results but the Shear-Stress Transport (SST)

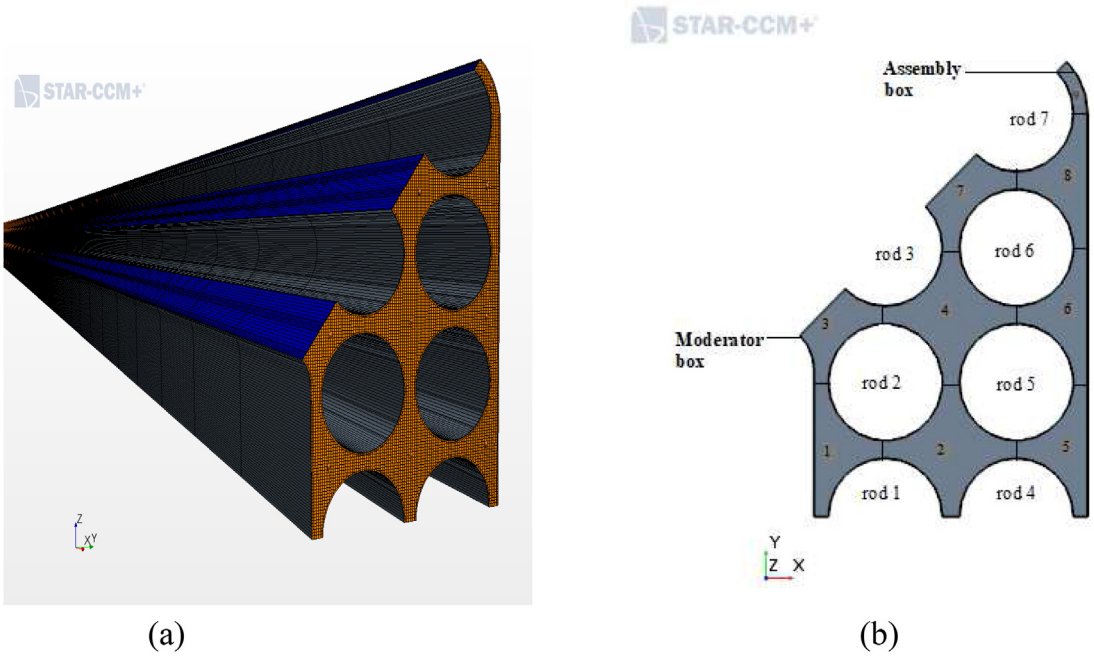

Fig. 1. Mesh Scene of the Computational Geometry (a), and a representation of Fuel rod and sub-channels in "1/8 assembly type square 2.1" (b) created using STAR CCM + CAD [19].

Table 1
Dimensions used for creating a 1/8th FA geometry [19].

Square "2.1" Assembly type	Values
Number of moderator boxes per assembly (−)	1
Cladding outer diameter	8 mm
P/D	9.2
Number of fuel rods (−)	40
Active axial heated height	4.2 m
Fuel assembly box	
Length of the inner side	65.2 mm
Thickness of wall	1 mm
Length of the outer side	67.2 mm
Moderator box	
Length of the outer side	26.8 mm
Thickness of wall	0.3 mm
Length of the inner side	26.2 mm

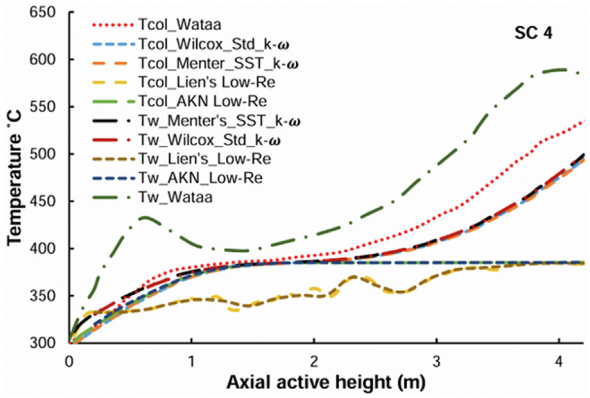

Fig. 2. Temperature profiles in SC 4 of a square fuel assembly [19].

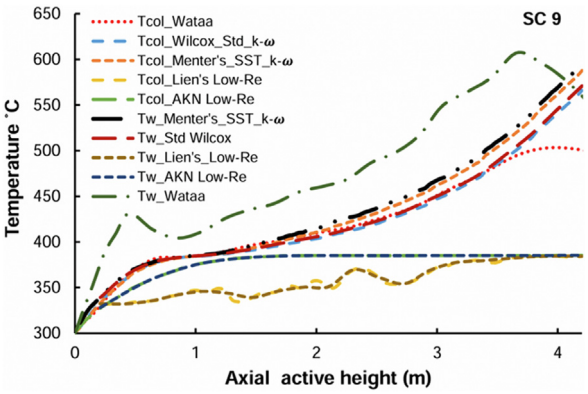

Fig. 3. Temperature profiles in SC 9 of a square fuel assembly [19].

Menter's, κ-ω was selected for the various numerical simulations in this work because of the wide recommendations made about this turbulence model in literature being suitable for predicting heat transfer at supercritical pressures. Thus results of Tw and Tcol temperatures produced by SST Menter's, κ-ω turbulence model using the STAR-CCM + code agree with that of Wataa's results using STAFAS code and hence these results used as means of validation of the numerical results obtained in this study due to unavailability of experimental data on the proposed HPLWR fuel assembly geometry used for the study.

3.2. Parametric analysis in sub-channels 4 and 9

Parametric trends for effects of varying the mass flow rate, operating pressure and gravity on the temperature distribution along the active height of the 1/8th fuel assembly to capture the heat transfer phenomena are evaluated and presented. Wall

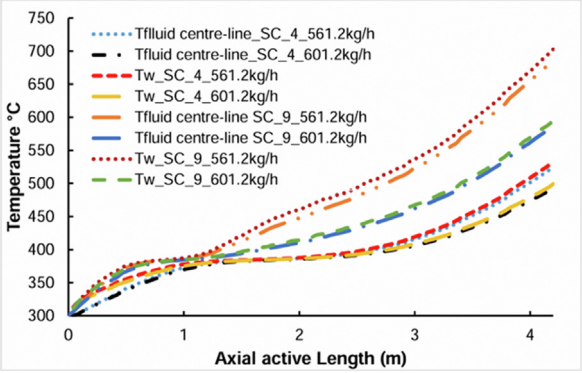

Fig. 4. Influence of Mass flow rate at 25 MPa in SCs (4) and (9).

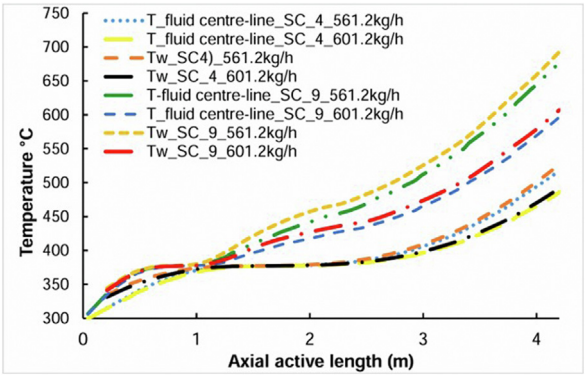

Fig. 5. Influence of Mass flow rate at 23 MPa in SCs (4) and (9).

Temperature (Tw) and Coolant or Fluid Temperature (Tcol or Tfluid) distribution results in sub-channels 4 and 9 (SC (4) and SC (9)) are presented in analyzing the effects of system mass flow rate, pressure and gravity on fluid flow and heat transfer in the sub-channels. SC (4) is located at the center of the fuel assembly (Central sub-channel) whereas SC (9) is located at the corner of the fuel assembly (Corner sub-channel) (see Fig. 1).

3.2.1. The influence of mass flow rate

The influence of mass flow rate at both 25 MPa and 23 MPa (with pseudo-critical temperatures of 384.9 °C and 377.5 °C respectively) on heat transfer phenomenon are illustrated in Fig. 4 and Fig. 5 respectively.

The analysis was carried out at mass flow rates of 0.1670 kg/s (601.2 kg/h) and 0.1559 kg/s (561.2 kg/h), 300 °C as inlet temperature and 650 kW/m^2 heat flux. The profiles of wall temperature values at 25 MPa and 23 MPa were obtained for normal heat transfer (NHT), enhanced heat transfer (EHT) and the deteriorated heat transfer (DHT) regions in Fig. 4 for 25 MPa and Fig. 5 for 23 MPa. Consider Fig. 4, in the NHT region of sub-channel 4 the wall temperature values for the 561.2 kg/h mass flow rate were larger than that of the 601.2 kg/h. However, in the enhanced heat transfer region the wall temperature values were almost equal for all the two mass flow rates of the system at 25 MPa. In the DHT region the wall temperature values for 561.2 kg/h mass flow rate were larger than that of the 601.2 kg/h mass flow rate. A similar trend of wall temperature values was observed in sub-channel 9 for the enhanced and deteriorated heat transfer regions. In the NHT region, the obtained wall temperature values for all the two mass flow rates at 25 MPa were almost same.

On the other hand, it was observed that both fluid centre-line temperature values for all the two mass flow rates in sub-channel 4 increased “linearly” below and beyond the pseudo-critical region, while in the pseudo-critical region the fluid centre-line temperature flattened. That is the fluid/coolant temperature increases below the pseudo-critical region, flattened at the pseudo-critical region (coolant temperature almost equals to the pseudo-critical point temperature value) and increases thereafter the pseudo-critical region. The fluid centre-line temperature values for the 561.2 kg/h were higher than that of the 601.2 kg/h but almost the same in the pseudo-critical region in both sub-channels at 25 MPa. At 25 MPa, the highest wall temperature obtained is 703.03 °C in SC (9) at the smaller mass flow rate of 561.2 kg/h while the least wall temperature obtained is 499.34 °C in SC (4) at the larger mass flow rate of 601.2 kg/h. The corresponding values of fluid centre-line temperature values are 687.37 °C in SC (9) and 493.69 °C in SC (4).

Fig. 5 shows the similar trend of the temperature distribution in the two SCs (4) and (9) at 23 MPa. At 23 MPa, the highest wall temperature obtained is 692.88 °C in SC (9) at the smaller mass flow rate of 561.2 kg/h while the least wall temperature obtained is 491.63 °C in SC (4) at the larger mass flow rate of 601.2 kg/h. The corresponding values of fluid centre-line temperature values are 670.07 °C in SC (9) and 486.12 °C in SC (4). Comparing the fluid/coolant and wall temperatures for the two mass flow rates of 601.2 kg/h and 561.2 kg/h at 25 MPa and 23 MPa, the fluid and wall temperatures obtained at the smaller mass flow rate were larger than those obtained at the larger mass flow rate. Similar finding was obtained by Refs. [8,9,16].

3.2.2. The influence of pressure

Fig. 6 and Fig. 7 respectively show the effect of varying the two system pressures 25 MPa and 23 MPa at two mass flow rates of 601.2 kg/h and 561.2 kg/h on heat transfer behaviour in the sub-channels of the fuel assembly based on the fluid centre-line temperature and wall temperature.

The simulation results showed that the general trend pattern of the wall and fluid centre-line temperatures under the two different mass flow rates (601.2 kg/h and 561.2 kg/h) behaved almost the same. Nevertheless, in Fig. 6, below the pseudo-critical region the fluid centreline temperature values for 23 MPa and 25 MPa in sub-channel 4 at 601.2 kg/h mass flow rate were almost the same. However, in and beyond the pseudo-critical region the values of fluid centerline temperature for 25 MPa are relatively larger than that of 23 MPa in sub-channel 4. A similar trend was observed in sub-channel 9 below the pseudo-critical region and in the pseudo-critical region, but beyond pseudo-critical region the values of the fluid centre-line temperature for 23 MPa are larger than that of the 25 MPa.

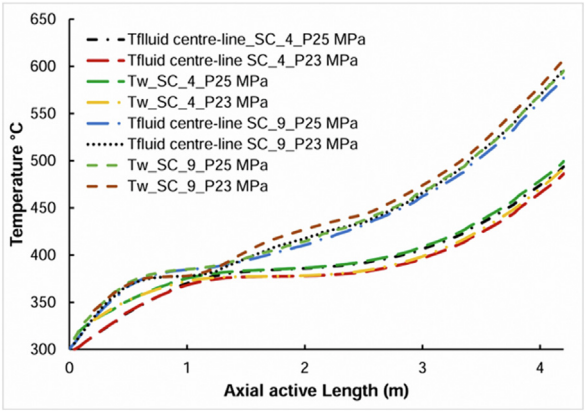

Fig. 6. Influence of pressure at 0.1670 kg/s (601.2 kg/h) in SCs (4) and (9).

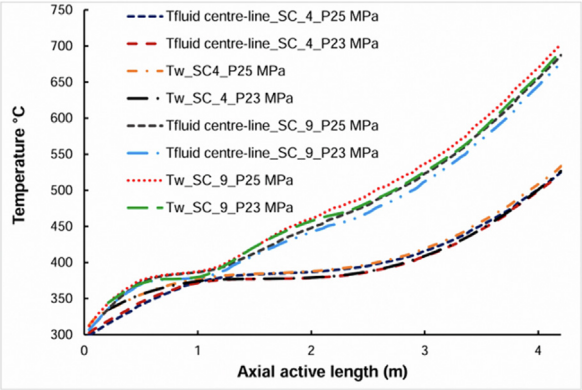

Fig. 7. Influence of pressure at 0.1559 kg/s (561.2 kg/h) in SCs (4) and (9).

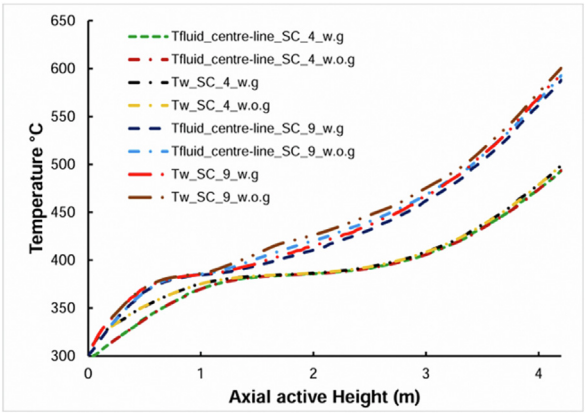

Fig. 8. Influence of gravity at 25 MPa (at mass flow rate of 0.1670 kg/s (601.2 kg/h)) in SCs (4) and (9).

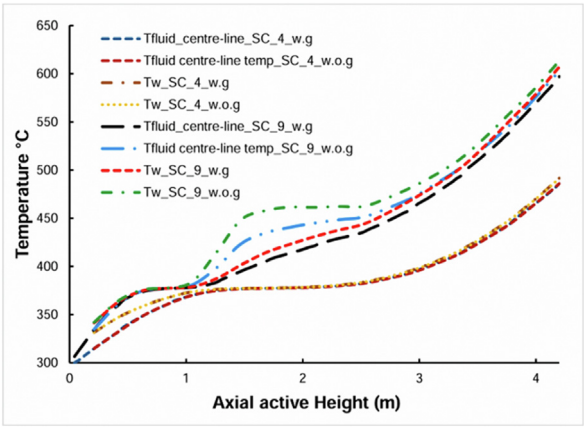

Fig. 9. Influence of gravity at 23 MPa (at mass flow rate of 0.1670 kg/s (601.2 kg/h)) in SCs (4) and (9).
N.B: w.g is with gravity and w.o.g is without gravity

At 561.2 kg/h in sub-channel 4 of Fig. 7, the values of the fluid centre-line temperature below the pseudo-critical region for both 23 MPa and 25 MPa were almost the same, while in the pseudo-critical region the fluid centre line temperature values for 25 MPa were relatively larger as compared to that of 23 MPa. Beyond pseudo-critical region the values of the fluid centre-line temperature for 25 MPa are slightly larger as compared to that of 23 MPa and became almost the same towards the exit of the sub-channel. In sub-channel 9, the values of the fluid centre-line temperature for 23 MPa and 25 MPa below pseudo-critical region were almost the same, while in the pseudo-critical region and beyond the pseudo-critical region the values of the fluid centre-line temperature for 25 MPa were relatively larger as compared to that of the 23 MPa.

The three heat transfer regimes NHT, HTE and HTD were observed for wall temperature values at both working pressures. It was observed that pressure had no effect in the normal heat transfer region at both 601.2 kg/h and 561.2 kg/h mass flow rates. The wall temperature values in the EHT region increased with pressure for all the two mass flow rates. In sub-channel 4, the wall temperature values for 25 MPa were relatively larger as compared to that of the 23 MPa in the enhanced and deteriorated heat transfer regions at 601.2 kg/h and 561.2 kg/h. In sub-channel 9, the wall temperature values in the EHT region for 25 MPa were relatively larger as compared to that of the 23 MPa for both mass flow rates. However, in the DHT region a different trend of wall temperature values was observed, at 601.2 kg/h the wall temperature values for 23 MPa were larger than that of 25 MPa. But at 561.2 kg/h the wall temperature values for 25 MPa were significantly larger as compared to that of the 23 MPa. It could also be observed that temperature distributions (fluid and wall) in sub-channel 9 were larger than those in sub-channel 4. The finding that temperature distributions obtained at higher system pressure were larger than those obtained at lower system pressure was also obtained by Refs. [9,16].

3.2.3. *The influence of gravity*

Fig. 8 and Fig. 9 show the influence of gravity on heat transfer based on the wall and fluid centre-line temperature profiles. The analysis was conducted at 25 MPa and 23 MPa working pressures, 300 °C inlet temperature and mass flow rate of 601.2 kg/h.

At both 25 MPa and 23 MPa almost equivalent trends and values for wall temperature for the normal heat transfer, enhanced and deteriorated heat transfer regions were obtained for the systems with or without gravity in sub-channel 4. But in sub-channel 9 the wall temperature values for the system without gravity effect were moderately larger as compared to the one with gravity effect in the deteriorated heat transfer region at both 25 MPa and 23 MPa. The occurrence of recovery from deteriorated heat transfer region was observed in the system without gravity at 23 MPa. On the other hand, the trends and values of the fluid centre line temperatures for the two systems were almost the same in sub-channel 4, but in sub-channel 9 the fluid centre line temperature for a system without gravity was larger than the one with gravity beyond pseudo-critical region.

It was also observed that the values of the fluid centre line temperature below and beyond the pseudo-critical region increased linearly, but flattened at the pseudo-critical region. The effect of gravity was more pronounced in sub-channel 9 than in sub-channel 4 at both working pressures of 25 MPa and 23 MPa. Also, the fluid and wall temperature values were relatively larger for system without gravity effect when compared with the system with gravity effect in sub-channel 9. Similar finding was obtained by Ref. [24].

It can be observed that at varying mass flow rate at constant pressure or at varying system pressure at constant mass flow rate, similar trends of positive linear gradients were obtained for wall temperature profiles in the NHT regions below the EHT regions. Similar trends of positive linear gradients were also obtained for wall temperature profiles in the DHT regions beyond the EHT regions. Similar wall temperature profiles with positive linear gradients were obtained in the NHT and DHT regions for influence of

gravity with varying system pressure at constant mass flow rate except that the occurrence of recovery from deteriorated heat transfer region was observed in the system without gravity at 23 MPa.

Consequently, based on the parametric analysis carried out, sub-channel 4 performed better in terms of heat transfer because temperatures predicted in sub-channel 9 (corner sub-channel) were higher than the ones obtained in sub-channel 4 (central sub-channel). The influence of system mass flow rate, pressure and gravity seem similar in both sub-channels 4 and 9 with temperature distributions higher in sub-channel 9 than in sub-channel 4. In most of the cases considered, temperature distributions (fluid and wall) obtained at 25 MPa are higher than those obtained at 23 MPa, temperature distributions obtained at 601.2 kg/h are higher than those obtained at 561.2 kg/h, and temperature distributions obtained without gravity effect are higher than those obtained with gravity effect.

4. Conclusion

The STAR-CCM + CFD code was used to simulate flow and heat transfer behaviour of supercritical water in the nine (9) sub-channels of 1/8th fuel assembly of which results on low temperature sub-channel 4 and high temperature sub-channel 9 are presented in this study for parametric analysis. Four selected turbulence models were assessed and tested namely, AKN $\kappa-\varepsilon$, Lien's Lo-Re $\kappa-\varepsilon$, standard (Wilcox) κ-ω and SST $\kappa-\omega$. Among the four assessed turbulence models, the Standard (Wilcox) κ-ω and SST $\kappa-\omega$ turbulence models captured closely Wataa's coolant and wall temperature distributions in the sub-channels. However, the SST κ-ω model was chosen to carry out the numerical simulations because SST κ-ω turbulence model is widely used and recommended by many researchers in studying heat transfer phenomena of supercritical fluids.

Results obtained from the parametric analysis in the two adopted sub-channels (sub-channels 4 and 9) showed that the fluid centre-line temperature linearly increased below and above the pseudo-critical region, but flattened at the pseudo-critical region for all the system parameters considered. The mass flow rate, pressure and gravity have effects on the wall temperature values in the normal heat transfer (NHT) region, enhanced heat transfer (EHT) region and deteriorated heat transfer (DHT) region. The variation of the system parameters (mass flow rate and gravity) in the enhanced heat transfer and pseudo-critical regions showed no significant difference in the wall temperature and fluid centre-line temperature values. However, for the pressure parameter a significant difference in the wall temperature and fluid centre-line temperature values was observed. The wall and fluid centre line temperature values increased with pressure in these regions (enhanced heat transfer and pseudo-critical regions). It can be observed that at varying mass flow rate at constant pressure or at varying system pressure at constant mass flow rate, similar trends of positive linear gradients were obtained for wall temperature profiles in the NHT regions below the EHT regions. Similar trends of positive linear gradients were also obtained for wall temperature profiles in the DHT regions beyond the EHT regions. Similar wall temperature profiles with positive linear gradients were obtained in the NHT and DHT regions for influence of gravity with varying system pressure at constant mass flow rate except that the occurrence of recovery from DHT region was observed in the system without gravity at 23 MPa.

Based on the parametric analysis carried out, sub-channel 4 performed better in terms of heat transfer because temperatures predicted in sub-channel 9 (corner sub-channel) were higher than the ones obtained in sub-channel 4 (central sub-channel). The influence of system mass flow rate, pressure and gravity seem similar in both sub-channels 4 and 9 with temperature distributions higher in sub-channel 9 than in sub-channel 4. In most of the cases considered, temperature distributions (fluid and wall) obtained at 25 MPa are higher than those obtained at 23 MPa, temperature distributions obtained at 601.2 kg/h are higher than those obtained at 561.2 kg/h, and temperature distributions obtained without gravity effect are higher than those obtained with gravity effect. This numerical study was not quantitatively compared with experimental data along the axial active heights of the sub-channels. Nonetheless, it was observed that the adopted numerical tool STAR-CCM + CFD code showed capabilities of capturing the trends for the normal heat transfer, enhanced and deteriorated heat transfer regions. Accordingly, from the deduced findings, experimental investigation should be carried out to validate the results and ascertain the applicability of the SST κ-ω turbulence model in heat transfer predictions at supercritical conditions in SCWR fuel assembly.

Declaration of competing interest

Dear Editor: Please find attached for your kind review our manuscript entitled “Heat transfer analysis in Sub-channels of Rod Bundle Geometry with Supercritical Water”.

The submitted manuscript for review has no conflict of interest in one form or the other in relation to similar research studies in the literature.

Acknowledgements

The authors are very grateful to Cd-Adapco for making it possible for the STAR-CCM + CFD code to be used at a reduced license fee. Prof. Walter Ambrosini of University of Pisa is also acknowledged for his technical support in developing cubic spline program which makes it possible for water and other coolants properties to be obtained.

References

[1] M.M. Rahman, J. Dongxu, N. Jahan, M. Salvatores, J. Zhao, Design concepts of supercritical water-cooled reactor (SCWR) and nuclear marine vessel: a review, Prog. Nucl. Energy 124 (2020) 103320.
[2] L. Castro, J.-L. François, C. García, Coupled Monte Carlo-CFD analysis of heat transfer phenomena in a supercritical water reactor fuel assembly, Ann. Nucl. Energy 141 (2020) 107312.
[3] X. Hao, P. Xu, H. Suo, L. Guo, Numerical investigation of flow and heat transfer of supercritical water in the water-cooled wall tube, Int. J. Heat Mass Tran. (2019), https://doi.org/10.1016/j.ijheatmasstransfer.2019.119084.
[4] Z. Zhang, C. Zhao, X. Yang, P. Jiang, J. Tu, S. Jiang, Numerical study of the heat transfer and flow stability of water at supercritical pressures in a vertical tube, Nucl. Eng. Des. 325 (2017) 1–11.
[5] Z. Shen, D. Yang, S. Wang, W. Wang, Y. Li, Experimental and numerical analysis of heat transfer to water at supercritical pressures, Int. J. Heat Mass Tran. 108 (2017) 1676–1688.
[6] M. Jaromin, H. Anglart, A numerical study of heat transfer to supercritical water flowing upward in vertical tubes under normal and deteriorated conditions, Nucl. Eng. Des. 264 (2013) 61–70.
[7] G. Zhang, H. Zhang, H. Gu, Y. Yang, X. Cheng, Experimental and numerical investigation of turbulent convective heat transfer deterioration of supercritical water in vertical tube, Nucl. Eng. Des. 248 (2012) 226–237.
[8] W. Gang, J. Pan, Q. Bi, Z. Yang, H. Wang, Heat transfer characteristics of supercritical pressure water in vertical upward annuli, Nucl. Eng. Des. 273 (2014) 449–458.
[9] H. Wang, Q. Bi, L. Wang, H. Lv, L.K.H. Leung, Experimental investigation of heat transfer from a 2×2 rod bundle to supercritical pressure water, Nucl. Eng. Des. 275 (2014) 205–218.
[10] M. Qu, D. Yang, Z. Liang, L. Wan, D. Liu, Experimental and numerical investigation on heat transfer of ultra-supercritical water in vertical upward tube under uniform and non-uniform heating, Int. J. Heat Mass Tran. 127 (2018) 769–783.
[11] Z. Gao, J. Bai, Numerical analysis on non-uniform heat transfer of supercritical pressure water in horizontal circular tube, Appl. Therm. Eng. 120 (2017) 10–18.

[12] F. Li, B. Bai, Flow and heat transfer of supercritical water in the vertical helically-coiled tube under half-side heating condition, Appl. Therm. Eng. 133 (2018) 512–519.
[13] H.B. Li, M. Zhao, Z.X. Hu, H.Y. Gu, D.H. Lu, Experimental study on transient heat transfer across critical pressure in 2×2 rod bundle with wire wraps, Int. J. Heat Mass Tran. 110 (2017) 68–79.
[14] H.Y. Gu, H.B. Li, Z.X. Hu, D. Liu, Heat transfer to supercritical water in a 2× 2 rod bundle, Ann. Nucl. Energy 83 (2015) 114–124.
[15] J. Chen, Z. Xiong, Y. Xiao, H. Gu, Experimental study on the grid-enhanced heat transfer at supercritical pressures in rod bundle, Appl. Therm. Eng. 156 (2019) 299–309.
[16] H. Lv, Q. Bi, X. Dong, Z. Zhang, G. Zhu, Investigation on heat transfer of in-tube supercritical water cooling accompanying out-tube pool boiling, Int. J. Heat Mass Tran. 136 (2019) 938–949.
[17] S. Chen, H. Gu, M. Liu, Y. Xiao, D. Cui, Experimental investigation on heat transfer to supercritical water in a three rod bundle with spacer grids, Appl. Therm. Eng. 164 (2020) 114466.
[18] S.E.-D. El-Morshedy, S.M.A. Ibrahim, A. Alyan, A. Abdelmaksoud, Heat transfer deterioration mechanism for water at supercritical pressure, International Journal of Thermofluids 7–8 (2020) 100020.
[19] S.K. Debrah, E. Shitsi, S. Chabi, N. Sahebi, Assessment of heat transfer correlations in the sub-channels of proposed rod bundle geometry for supercritical water reactor, Heliyon 5 (2019), e02927.
[20] K. Podila, Y.K. Rao, CFD analysis of flow and heat transfer in Canadian supercritical water reactor bundle, Ann. Nucl. Energy 75 (2014) 1–10.
[21] CD-ADAPCO, User Guide STAR-CCM+, 2015. Version 10.06.009", New York.
[23] X. Xi, Z. Xiao, X. Yan, T. Xiong, Y. Huang, Numerical simulation of the flow instability between two heated parallel channels with supercritical water, Ann. Nucl. Energy 64 (2014b) 57–66.
[24] E. Shitsi, S.K. Debrah, V.Y. Agbodemegbe, E. Ampomah-Amoako, Numerical investigation of heat transfer in parallel channels with water at supercritical pressure, Heliyon 3 (11) (2017), e00453.
[25] C.L. Waata, Coupled Neutronics/Thermal-Hyhdraulics Analysis of a High Performance Light Water Reactor Fuel Assembly, PhD Thesis, 2006, p. 104.
[26] Zhirui Zhao, Yitung Chen, Baozhi Sun, Jianxin Shi, Xiang Yu, Wanze Wu, Non-uniform thermal-hydraulic behavior in a 61-rod bundle of supercritical water-cooled reactor, Appl. Therm. Eng. 171 (2020), https://doi.org/10.1016/j.applthermaleng.2019.114688, 114688.